Journal of the Serbian Chemical Society
JSCS-info@shd.org.rs • www.shd.org.rs/JSCS
J. Serb. Chem. Soc. 81 (5) 589–605 (2016)
JSCS–4870
UDC 678.742+547.458.81+546.723'722: 539.216
Original Scientific paper

A study of the barrier properties of polyethylene coated with a nanocellulose/magnetite composite film

NENAD ĐORĐEVIĆ[1], ALEKSANDAR D. MARINKOVIĆ[2#], JASMINA B. NIKOLIĆ[2#], SAŠA Ž. DRMANIĆ[2#], MILICA RANČIĆ[3#], DANIJELA V. BRKOVIĆ[4]* and PETAR S. USKOKOVIĆ[1#]

[1]*Department of Graphic Engineering, Faculty of Technology and Metallurgy, University of Belgrade, Karnegijeva 4, 11120 Belgrade, Serbia,* [2]*Department of Organic Chemistry, Faculty of Technology and Metallurgy, University of Belgrade, Karnegijeva 4, 11120 Belgrade, Serbia,* [3]*Faculty of Forestry, University of Belgrade, Kneza Višeslava 1, 11030 Belgrade, Serbia and* [4]*Innovation Center, Faculty of Technology and Metallurgy, University of Belgrade, Karnegijeva 4, 11120 Belgrade, Serbia*

(Received 17 December 2015, revised 10 February, accepted 11 February 2016)

Abstract: The morphological, thermal and barrier properties of low-density polyethylene/polycaprolactone-modified nanocellulose hybrid materials were investigated in this study. Nanocellulose/magnetite (NC–Fe_3O_4) nanocomposite and maleic acid functionalized NC/magnetite (NCMA–Fe_3O_4) nanocomposite were prepared and used as fillers at various concentrations (5, 10 and 15 wt. %) in the polycaprolactone (PCL) layer. PE was coated with a PCL/NC/ /magnetite layer. The addition of the filler did not unfavorably affect the inherent properties of the polymer, especially its barrier properties. Oxygen permeation measurements showed that the oxygen barrier properties of magnetite enriched PCL film were improved due to the chemical activity of the added material. The highest level of the barrier capacity was observed for PE samples coated with a PCL-based composite with NCMA–Fe_3O_4 micro/nanofiller, which implies a significant contribution of the surface modification of the nanocellulose with maleic anhydride residue to the improved barrier properties.

Keywords: hybrid materials; composites; inorganic filler; polycaprolactone; packaging material.

INTRODUCTION

Since packaging in recent times represents the largest market for the consumption of plastic material, thus creating many problems concerning post-

* Corresponding author. E-mail: dbrkovic@tmf.bg.ac.rs
# Serbian Chemical Society member.
doi: 10.2298/JSC151217019D

consumption disposal of wastes, there is an increasing interest for the development of new biodegradable materials instead of petroleum-based polymers for packaging applications. On the other hand, the involvement of nanotechnology in food packaging is growing following the increasing demand for improved barrier, mechanical, antimicrobial properties and the incorporation of nanosensors for the monitoring of food condition during transport.[1] One of the most important issues in food packaging is the migration and permeability of oxygen and carbon dioxide, water vapor, or natural substances contained in the food or the packaging material. Although in some applications, high gas barrier properties are undesirable, such as in the packaging for fresh fruits and vegetables, the shelf life of which is dependent on access to a continual supply of oxygen for sustained cellular respiration.[2] A lot of effort has recently been spent on developing new high performance nanocomposite films for packaging applications with a polymer matrix and nanofillers that are completely renewable. Nanocellulose (NC), as most abundant biopolymer in nature, represents a remarkable emerging class of nature-derived nanomaterials because of its biodegradibility, extraordinary mechanical properties, high stiffness of up to 140 Gpa, lightweight character (density *ca*. 1.5 g cm^{-3}), as well as diversity of potential chemical modifications.[3–5] Cellulose nanocrystals (CNCs) can be produced from acid hydrolysis of various natural cellulose sources, such as cotton, cellulose fibers from lignocellulosic materials and a marine animal tunicate.[6,7] In order to expand the use of nanocellulose as a gas barrier in high-moisture environments, its hydrophilicity must be decreased by chemical modification of its surface.[8]

During the last years, CNCs have been used as reinforcing fillers in other polymer materials for improving barrier,[2,9,10] mechanical[10–12] and other properties, but only few researches focused on cast CNCs coatings. For example, Li *et al.* reported the multifunctional and uniform coating of CNCs (extracted from cotton linter) onto polyethylene terephthalate (PET), oriented polypropylene (OPP), oriented polyamide (OPA) and cellophane films for better performance for flexible packaging applications that showed excellent anti-fog and remarkable oxygen barrier properties, reducing the coefficient of friction while maintaining higher transparency (≈90 %) and low haze values (3–4 %). CNCs-coated PET and OPA showed the best performance among the investigated coated films.[13]

Despite its high strength, light weight, water resistance and great stability that make it a good candidate for food packaging material,[14] the largest disadvantages of commercial low density polyethylene (PE) are reflected in its oxygen, carbon dioxide, organic vapor and water vapor permeability. Modification of the surface of PE has been proven an effective way to improve the performance of the material and to enhance its barrier and mechanical properties. In this work, the mechanical and barrier properties of nanocomposite films made of modified

cellulose nanocrystals (CNCs) and those coated onto polyethylene (PE) foil were investigated.

Different metal oxides have been widely used as fillers in order to reduce water vapor permeability and enhance antibacterial, mechanical or magnetic properties of various polymers.[15,16] Magnetite has mostly been used as a filler for improving LDPE super-paramagnetic properties and to prepare flame-retardant low-density polyethylene.[17,18] Investigations dealing with the influence of magnetite or nanocellulose–magnetite composites on the barrier properties of LDPE have, to best of our knowledge, not been published in the literature.

In this study, PE was coated with a thin film of differently modified nanocellulose, while PCL was used as a binder to enhance the compatibility at the interface of PE/modified nanocellulose composites. This procedure was performed in order to improve the previously mentioned functional properties of packaging material while maintaining the health and safety requirements.

EXPERIMENTAL

Materials

All chemicals used in this study were reagent grade or p.a. quality, and used as received. Deionized water (DW), resistivity of 18 MΩ cm, was used as solvent and for glassware washing. The chemicals were purchased from different suppliers: sulfuric acid and perchloric acid (Sigma); ammonia (Zorka Pharma); poly(*N*-vinyl pyrrolidone) (PVP, Kollidon 90, BASF); maleic anhydride, $FeCl_3 \cdot 6H_2O$ and $FeSO_4 \cdot 7H_2O$ (Merck), polycaprolactone, (average molecular weight of ≈45000 g mol^{-1}, copper(II) acetate, tetrahydrofuran (THF), toluene, methanol, dicloromethane and chloroform (Sigma–Aldrich). Polyethylene foil LG SP 311 (LLDPE) was supplied by Macchi (three-layer folio 28/44/28%).

Preparation procedures

Preparation of nanocellulose (NC). Nanocellulose nanocrystals (NC) were prepared from commercially available cellulose by acid hydrolysis with sulfuric acid according to an established procedure.[19] Thus, about 20 g of cotton was mixed with 200 mL sulfuric acid (64 wt. %), the mixture was hydrolyzed at 40 °C for 60 min under continuous stirring. The hydrolysis was quenched by the addition of 1000 mL of water to the reaction mixture and the slurry was centrifuged for 20 min at 5000 rpm. The supernatant was removed and the pellet was washed with deionized water in successive sonification and centrifugation steps until the pH value of the supernatant became 4 or it became turbid. The final wash involved dialysis against deionized water until the wash water maintained a constant pH of 5.

Chemical modification of nanocellulose with maleic anhydride (NCMA). Subsequently, NC was modified by esterification with maleic anhydride according to a slightly modified literature method.[20] In order to change the solvent for the chemical modification of nanocellulose, the obtained cellulose nanoparticles were washed with acetic acid. A sample of 20 g of nanocellulose was prepared for modification with maleic anhydride (Fig. 1) by alternately washing and centrifuging with acetic acid three times in order to exchange the solvent. The sample was placed in a stoppered glass bottle containing a mixture of 160 mL of acetic acid and 200 mL of toluene and homogenized in an ultrasonic bath (Bandelin Electronic, Berlin, Germany, power of 120 W and frequency of 35 kHz), sonicated for 1 min. After homogenization, 0.8 mL of 60 % perchloric acid was added, the reaction mixture was sonicated for 1

min, and then, 0.5 g of maleic acid anhydride was added. The mixture was allowed to stand for 1 h at room temperature. After the reaction, the NC sample was thoroughly washed and centrifuged with toluene, methanol and dichloromethane, sequentially.

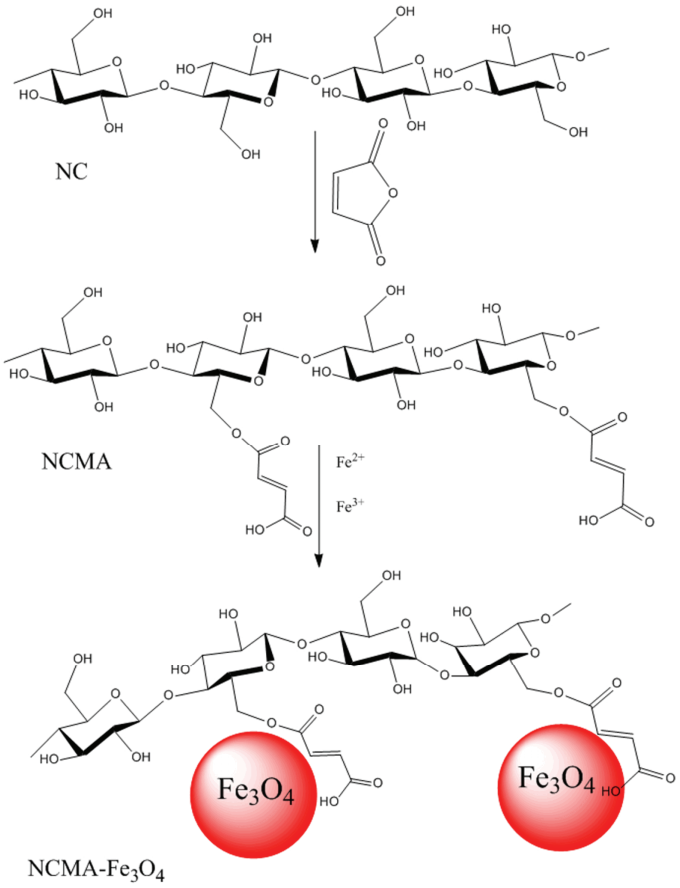

Fig. 1. Chemical modification of NC and preparation of magnetite nanocellulose composites (NC–Fe_3O_4 and NCMA–Fe_3O_4).

Preparation of magnetite nanocellulose composites (NC–Fe_3O_4 and NCMA–Fe_3O_4). Magnetite nanocellulose composites (Fig. 1) were prepared by co-precipitation of Fe(II) and Fe(III) ions in aqueous solutions containing NC or NCMA with ammonia according to a literature procedure.[17] In brief, 1.5 g of the nanocellulose sample (NC or NC–MA) was dispersed in 200 mL distilled water and stirred for 10 min. Then, 1.09 g $FeCl_3 \cdot 6H_2O$ and 0.765 g $FeSO_4 \cdot 7H_2O$ were added to the cellulose solution, which became orange. The mixture was heated to 60 °C and then 8.0 M ammonia solution was added dropwise. Vigorous stirring at a constant pH of 10 provided chemical precipitation of Fe_3O_4 onto the nanocellulose surface. The addition of ammonia solution caused the initial orange color to change to a black precipitate. The suspension was maintained at 60 °C under stirring for 4 h. After cooling to room temperature, the obtained NC–Fe_3O_4 and NCMA–Fe_3O_4 particles were separated magnetic-

ally, washed several times with DI water, then with ethanol and finally dried in a vacuum oven.[21]

Preparation of composite film on polyethylene surface (PE/nanocellulose composite). Polycaprolactone (PCL) solution were prepared by dissolving 16 g of PCL pellets in 120 mL of dry THF using a combination of both mixing and ultrasound treatment. Solutions of the nanocellulose-based nanofillers, NC, NC–Fe_3O_4, NCMA–Fe_3O_4, were prepared by dispersing appropriate amounts in 40 mL THF by homogenizing in three steps: mixing at 800 rpm for 30 min using a mechanical stirrer, ultrasound treatment for 15 min at 30–35 °C and grinding using an Ultra-turrax batch disperser at 12000 rpm for 5 min. The amounts of the nanofillers were calculated to give final concentrations of 5, 10 and 15 % based on PCL in the final solution. The PCL-based composite dispersions were immediately used for production of thin film on unmodified a PE surface by layering using an anilox roller with a 10 μm indentation (Fig. 2).

The compositions of the prepared barrier composite materials applied for coating PE are given in Table I.

TABLE I. Composition of the prepared barrier materials (BM); *x* is the content of nanofiller

Barrier material	Composition	*x* / wt. %
BM0	PE	–
BM1	PE + PCL	–
BM2	PE+PCL+NC	5
BM3		10
BM4		15
BM5	PE+PCL+NC–Fe_3O_4	5
BM6		10
BM7		15
BM8	PE+PCL+NCMA–Fe_3O_4	5
BM9		10
BM10		15

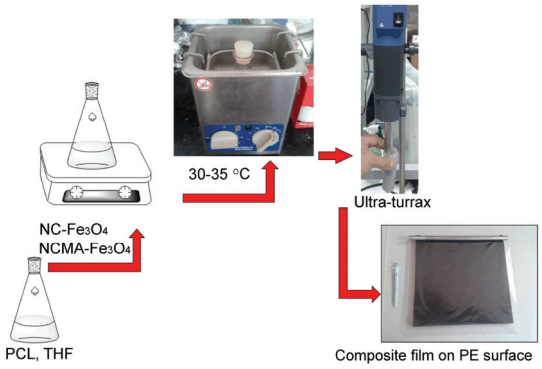

Fig. 2. Schematic presentation of the film preparation procedure.

Characterization methods

Fourier-transform infrared (FT–IR) spectra were recorded in the transmission mode between 400 and 4000 cm^{-1} using a BOMEM (Hartmann & Braun) spectrometer with a resolution of 4 cm^{-1}. X-Ray diffraction (XRD) data were obtained using a Bruker D8

Advance with a Vario 1 focusing primary monochromator (Cu $K_{\alpha 1}$ radiation, λ = 1.54059 Å). The XRD patterns were obtained over the Bragg angle (2θ) range of 10–90 °.

The textural properties were investigated by the Brunauer–Emmett–Teller (BET) and Barrett–Joyner–Halenda (BJH) methods using a Micromeritics ASAP 2020 surface area and porosity analyzer to obtain the specific surface area mesoporosity parameters, respectively.

Scanning electron microscopy (FEG-SEM) was performed with a field emission gun Tescan MIRA3 XMU electron microscope for recording the images of the surfaces of NC and the NC composites.

Thermogravimetric analysis (TGA) was performed using a Seteram Setsys Evolution--1750 instrument. The TGA experiments were run in a dynamic nitrogen atmosphere (flow rate 25 cm^3 min^{-1}) from 30 to 600 °C at a heating rate of 10 °the C min^{-1}.

The pH values at the point of zero charge (pH_{PZC}) of the samples, *i.e.* the pH above which the total surface of the samples is negatively charged, were measured using the pH drift method.[22]

The permeabilities of gases CO_2, N_2, O_2 and air were determined according to the DIN 53380 standard.[23] This standard is the universal testing method applicable to nearly all gases for the determination of the gas transmission rate through plastic films or other materials depending on temperature and the tested gas. This standard is an isostatic gas-chromatographic method using a Lyssy GPM-200 apparatus, gas chromatogram manufacturer Gasukuro Kogyo GC-320 and an HP 3396 integrator. The tests are performed at 23 °C and at a differential pressure of 1 bar. Samples of the film are fixed to a carrier and placed into an interrogation chamber. The permeability of gas is determined under isostatic conditions in a chamber divided into two parts by the film sample. Pure helium is in the chamber on one side of the film and a mixture of oxygen, nitrogen, carbon dioxide in the ratio of 1:1:1 is on the other side. The pressure on both sides is the same (0.2 bar). During the analysis, there is a gradual saturation of the helium gas, depending on the permeability of the film. The concentrations of the gases in the chamber with helium gas are detected on a chromatogram and integrator. The peak area on the obtained chromatogram at a given retention time is a function of time and represents the amount of permeate from the mixture. Air permeability is calculated based on the individual gases in the air. The results of the obtained gas permeability values are expressed in the units of cm^3 m^{-2} day^{-1} at 1 bar pressure difference.

RESULTS AND DISCUSSION

Although polymeric materials such as polyethylene are widespread due to their ease of processing, good properties and low cost, composite materials have many advantages compared to pure polymeric materials, *e.g.*, enhanced mechanical properties, reduced density or enhanced thermal properties. The properties of composite materials are significantly influenced by the properties of the individual components and may be adjusted by choosing the right type and amount of filler. Research and development of polymeric materials coupled with the appropriate filler, matrix–filler interaction and new formulation strategies to develop nanocomposites have led to potential applications in various types of packaging (agricultural products, dried food, frozen food, *etc.*).

In order to obtain new LDPE nanocomposite films with improved barrier properties for packaging applications, different polyethylene/polycaprolactone-

-modified nanocellulose hybrid materials were prepared. The morphological, thermal and barrier properties of obtained hybrid materials were investigated. Firstly, nanocelulose/magnetite (NC–Fe_3O_4) composite and maleic acid functionalized NC/magnetite (NCMA–Fe_3O_4) composite were prepared and used as filler at various concentrations (5, 10 and 15 wt. %) in a polycaprolactone (PCL) layer on the surface of polyethylene. A good distribution of the nanocellulose nanocomposites was achieved by dissolving it in polycaprolactone. Comprehensive experimental work through the multi-step synthesis of NC, NCMA, NC–Fe_3O_4 and NCMA–Fe_3O_4 was applied in order to design materials with an appropriate geometry, pore structure and magnetite deposit to obtain materials with improved barrier properties.

Textural properties and pH_{PZC}

The determined values of adsorbents textural properties and isoelectric points are summarized in Table II.

TABLE II. Textural properties, pH_{PZC} of NC, NCMA, NC–Fe_3O_4 and NCMA–Fe_3O_4

Adsorbent	Specific surface area $m^2\ g^{-1}$	Pore volume $cm^3\ g^{-1}$	Pore diameter nm	pH_{PZC}
NC	55.4	0.25	9.2	3.2
NCMA	52.3	0.29	10.4	4.1
NC–Fe_3O_4	72.1	0.44	14.2	6.5
NCMA–Fe_3O_4	89.2	0.51	15.2	6.2

The obtained textural parameters indicated higher volumes and pore diameters of NC–Fe_3O_4 and NCMA–Fe_3O_4 than for NC and NCMA, which could be attributed to the hybrid structure of the cellulosic/iron oxide composites. Additionally, the lower pH_{PZC} values, indicating an accumulation of negative charges on NC and NCMA, could have a beneficial to repelling effect. On the other hand, the higher surface area and pore volume of NC–Fe_3O_4 and NCMA–Fe_3O_4 contribute to a higher available surface area capable for interaction with diffusionally transported gases.

FTIR analysis

Fourier-transform infrared spectroscopy (FTIR) was employed to investigate the structural changes of NC and NC composites. The FTIR spectra of the unmodified and modified nanocellulose samples are shown in Fig. 3. The broad absorption band at 3440 cm^{-1} is due to the stretching vibrations of hydroxyl groups and the different intensities of the peak indicate the lower content in the NCMA sample, which is also the evidence of successful functionalization. The bands in the region of 3000–2800 cm^{-1} are assigned to the symmetric and antisymmetric stretching modes of C–H bonds in methyl (CH_3) and methylene

(CH_2) functional groups. The band observed at 2905 cm^{-1} corresponds to aliphatic saturated C–H stretching vibrations in cellulose.[21] The overlapped bands in the region of 1200–950 and formation of an intense signal with a center at 1069 cm^{-1} and multiple shoulders on both sides mainly belong to stretching modes of carbohydrate rings and side groups (C–OC, C–OH and C–H). Hydrolysis and reduction of the molecular weight of cellulose results in the appearance of a band at ≈1159 cm^{-1} and a shoulder at 1105 cm^{-1} assigned to C–C ring breathing and the C–O–C glycosidic ether group, respectively. These absorption bands are the consequence of gradual loss and decrease in molecular weight of the polysaccharide due to NC formation.[24] The absorption band at 894 cm^{-1} is attributed to C–H rocking vibrations, characteristic of β-glycosidic linkages between the glucose units in cellulose.[21]

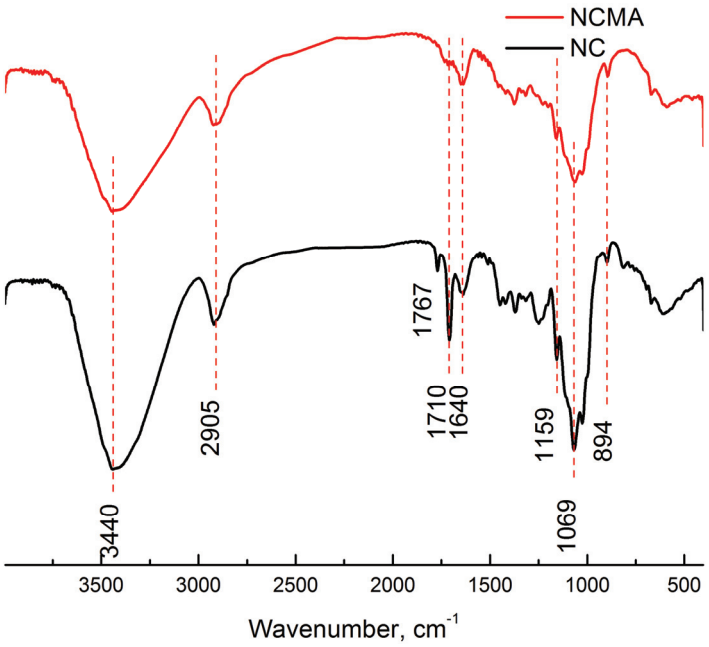

Fig. 3. FTIR spectra of NC and NCMA.

The FTIR spectra of NC–Fe_3O_4 and NCMA–Fe_3O_4, presented in Fig. 4, are very similar to those of NC and NCMA. Both spectra show absorption bands at around 3339, 2900 and 1635 cm^{-1} due to hydrogen bonded O–H stretching vibrations, C–H stretching from the methyl (CH_3) and methylene (CH_2) functional groups and –OH bending vibrations, respectively. The shift of the absorption band assigned to O–H stretching vibrations (from 3440 for NCMA to 3339 cm^{-1} for NCMA–Fe_3O_4) is probably due to interactions between the –OH groups from nanocellulose and the Fe_3O_4 particles. The most evident difference compared to

FTIR spectra of NC and NCMA is the appearance of a strong absorption band at 560 cm^{-1}, attributed to Fe–O in the tetrahedral sites.[21]

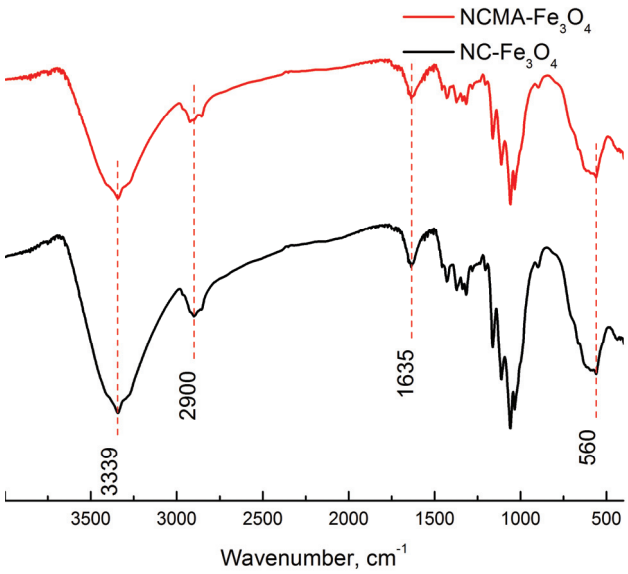

Fig. 4. FTIR spectra of NC–Fe_3O_4 and NCMA–Fe_3O_4.

X-Ray diffraction (XRD)

The recorded XRD patterns provide insight into the structural changes of the prepared NC composites. The diffractograms of NC and NCMA are shown in Fig. 5. An increase in crystallinity after modification of NC with maleic acid

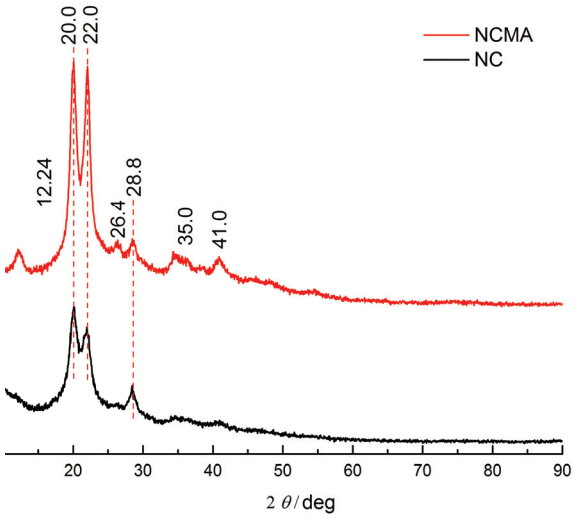

Fig. 5. XRD patterns of NC and NCMA.

anhydride was observed. Both diffractograms display a well-defined peak doublet at around 2θ 20 and 22° for the (200) plane of cellulose, which indicate the existence of cellulose I and cellulose II allomorphs, respectively.[25] Modification with maleic acid anhydride resulted in sharper signals, an increase in the contribution of cellulose II crystallites and an increase in the overall degree of crystallinity. Moreover, in the sample of NCMA, a signal at 12.5° was present.[26] The signal at 2θ 35.0°, having a higher intensity in the diffractogram of the NCMA sample, corresponds to the (004) atomic plane of cellulose I.[25]

The XRD patterns of the samples NC–Fe_3O_4 and NCMA–Fe_3O_4 are presented in Fig. 6. The distinct signals that appeared at 30.3°, 35.8°, 42.8°, 57° and 63° indicate the presence of pure Fe_3O_4 with a spinel structure.[21] A peak corresponding to cellulose I allomorphs was clearly visible and slightly shifted to a higher 2θ value (22.5°). The signal of cellulose II allomorphs was absent from both diffractograms, suggesting that precipitation of Fe_3O_4 particles favors the cellulose I allomorphs configuration of both the unmodified and modified nanocellulose.

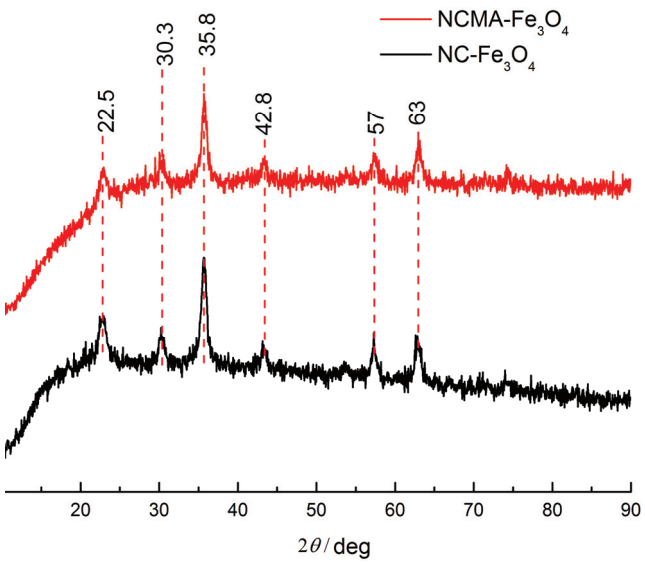

Fig. 6. XRD patterns of NC–Fe_3O_4 and NCMA–Fe_3O_4.

Thermogravimetry

The thermal stabilities of the unmodified and modified nanocellulose, and the prepared magnetite composites were investigated. Determination of residual iron oxide, *i.e.*, the quantitative determination of the magnetite loading, was studied using thermal gravimetric analysis (TGA). The TG curves of NC, NCMA, NC–Fe_3O_4 and NCMA–Fe_3O_4, are presented in Fig. 7. The similar trend

in thermal behavior of NC and NCMA samples could be observed. In both cases, a small weight loss (≈10 wt. %) in the temperature range <240 °C corresponding to desorption of adsorbed/crystallized water and defragmentation of the maleic acid residue from NCMA surface was detected. The weight loss in the temperature range 260–350 °C may be assigned to the thermal degradation of nanocellulose. In the second stage, almost 64 wt. % weight loss occurred due to the splitting/thermal decomposition of the cellulose structure, chain scission that leads to the evolution of gaseous products leaving a condensation/carbonaceous residues. After 440 °C, about 16 wt. % weight loss was observed due to the degradation of the condensed carbonaceous/residual organic material.

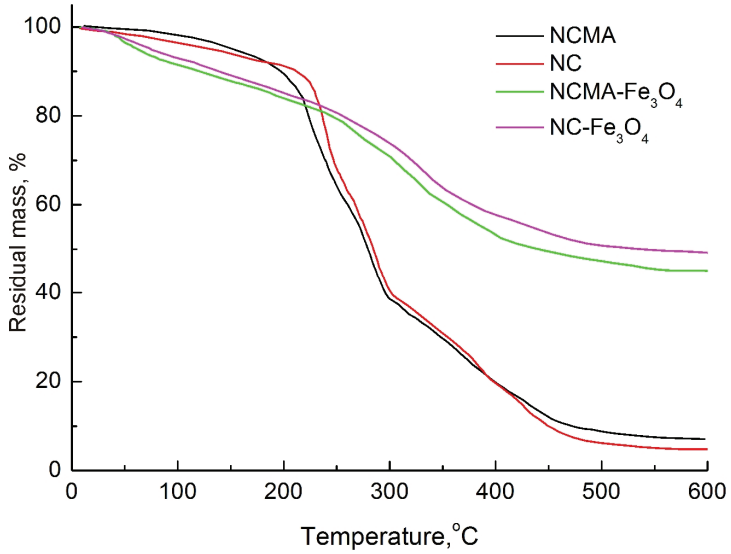

Fig. 7. Thermograms of NC, NCMA, NC–Fe_3O_4 and NCMA–Fe_3O_4.

The results show higher thermal stability of the NC and NCMA magnetite modified samples. Three degradation stages were found for NC–Fe_3O_4 and NCMA–Fe_3O_4: *i*) 50–300 °C, *ii*) 300–400 °C and *iii*) >400 °C. The first stage (≈22 % weight loss) corresponded to the gradual release of physically adsorbed and crystallized water, residual reactants on the NC surface (adsorbed mainly by hydrogen bonding) and slight decomposition of the cellulose chain. The second stage of decompositions (300–400 °C) of NC–Fe_3O_4 and NCMA–Fe_3O_4 were ascribed to the rapture of weak head-to-head acetal linkages between the cellobioze units in the amorphous/lower crystallinity domains of NC. The third stage, at temperatures above 400 °C, showed a weight loss of ≈18 % due to the random scission/gradual decomposition of the main polymeric chains of cellulose. Similar loadings of iron oxide (residual material) in the samples of NC–Fe_3O_4 and NCMA–Fe_3O_4 (49 and 47 wt. %, respectively) were observed.

Scanning electron microscopy

FE-SEM was employed in order to study the morphological changes of the NC composites. The SEM micrographs in Fig. 8 present unmodified NC, and the composites NC–Fe_3O_4 and NCMA–Fe_3O_4 (Figs. 8a–c, respectively). It could be concluded that the surface of NC, as well as NCMA was completely and uniformly coated with Fe_3O_4 particles. Those findings are in accordance with previously reported studies dealing with cellulose substrates covered by conductive particles.[27,28] The Fe_3O_4 particles in a form of platelets encapsulated nanocellulose, resulted in a uniform full coverage of the polymer surface.

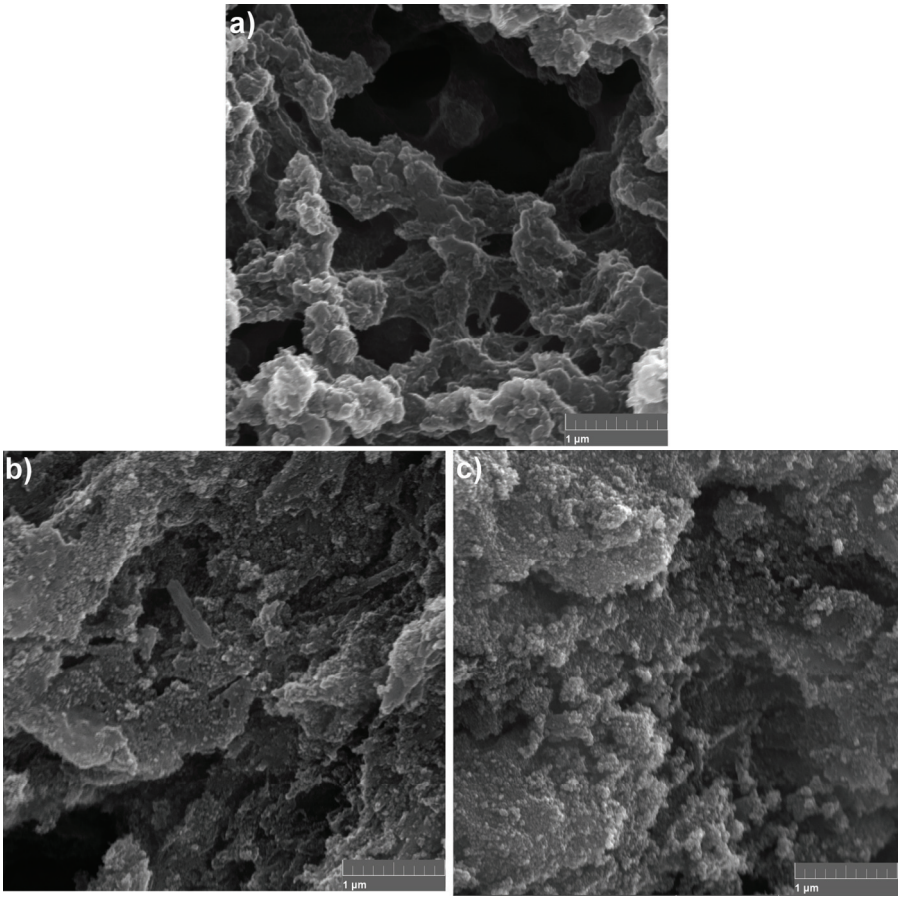

Fig. 8. SEM micrographs of: a) NC, b) NC–Fe_3O_4 and c) NCMA–Fe_3O_4.

Barrier properties

As mentioned previously, the goal of this work was to increase the barrier properties of bio-based materials in order to develop environmentally friendly

and efficient materials for packaging applications. In this regard, nanocellulose-based nanocomposites offer one the most promising prospects in the form of nanocomposite films. It is well known that high gas barrier properties are the most important limiting factors considered for modified atmosphere packaging. The higher is the degree of crystallinity, the higher are the barrier properties of the material. Despite the high barrier properties of nanocellulose, due to its high degree of crystallinity and the fact that nanocellulose exhibits oxygen barrier properties even much superior to those of cellophane,[29] very little research can be found in the literature concerning investigations of the barrier properties of nanocellulose and NC-based nanocomposites. Aulin *et al*. studied the oxygen barrier properties of cellulose microfibrils and explained the enhanced barrier properties of the MFC films against gases and vapors by the high-level of crystallinity and dense packing.[30] According to literature data,[31] the oxygen permeability for pure microfibrillated cellulose (MFC) films of 44 μm average thickness was 17/18.5 cm^3 m^{-2} d^{-1}. Other researchers obtained oxygen permeabilities four time lower (4.1/4.2 cm^3 m^{-2} d^{-1}) for doubled film thickness.[32] The recommended values for modified atmosphere packaging are 10–20 cm^3 m^{-2} d^{-1}.[33] It could be concluded that the film density is also an important variable in terms of the barrier properties of films. A composite material of high-density polyethylene and cellulose showed very good barrier properties towards oxygen. This was explained by the presence of impermeable cellulose crystals.[34] In this research, the initial thickness of the polyethylene film was 0.02 mm. The average mass and thickness of the PCL based composite film deposited on the PE surface was determined by both high precision weighing (gravimetric method) and automatic micrometer measurements. The results are listed in Tables III and IV, where the values of the barrier properties together with thickness of nanocomposite films are presented. The mass and thickness of the PCL layer increase with increasing concentration of the filler. The best barrier properties show sample BM10, with the highest content of NCMA–Fe_3O_4 (15 wt. %). Improved barrier properties of nanocomposite films can be explained by increasing of the crystal regions, which are impervious to water and gas transmission, conversely to the amorphous regions through which water and gas molecules diffuse easily. Additionally, the chemical modification of the nanocellulose increased the hydrophobicity. The oxygen permeability values seem to decrease with increasing film thickness, supporting the pore blocking theory, *i.e*., less connected pores throughout the film. If there are no pores allowing for gas flow through a material, the gas permeability will depend on the dissolution of oxygen and its rate of diffusion in the particular material.[31] The chemical reactions presented in Eq. (1)–(4) could occur in the barrier film and contribute to the decreased permeability of oxygen:

$$Fe \rightarrow Fe^{2+} + 2e^{-} \quad (1)$$

$$O_2 + 2H_2O + 4e^- \rightarrow 4OH^- \quad (2)$$

$$Fe^{2+} + 2OH^- \rightarrow Fe(OH)_2 \quad (3)$$

$$4Fe(OH)_2 + O_2 + 2H_2O \rightarrow 4Fe(OH)_3 \quad (4)$$

The presented redox reactions indicate that an appropriately designed system could significantly improve the barrier properties, due not only to physical barrier mechanism, but also to chemical consumption of the permeable oxygen that concomitantly produces a material with improved physical barrier properties.

TABLE III. Results of the barrier properties (gas permeability, cm^3 m^{-2} d^{-1} bar^{-1}) for pure polyethylene and the nanocellulose-based nanocomposite films, samples BM0–BM5

Gas	Barrier material					
	BM0	BM1	BM2	BM3	BM4	BM5
CO_2	98.41	84.95	81.54	78.32	75.91	79.23
O_2	35.33	34.01	31.56	28.88	27.21	29.88
N_2	13.94	13.87	12.97	11.86	10.92	12.22
Air	18.48	18.29	18.02	17.52	16.96	17.66
Film thickness	60	9	12	11	14	10

TABLE IV. Results of the barrier properties (gas permeability, cm^3 m^{-2} d^{-1} bar^{-1}) for the nanocellulose-based nanocomposites, samples BM6–BM10

Gas	Barrier material				
	BM6	BM7	BM8	BM9	BM10
CO_2	75.26	69.45	72.66	66.45	59.23
O_2	27.01	24.46	27.89	24.94	22.56
N_2	11.88	11.06	12.01	10.88	9.97
Air	16.44	15.38	18.38	15.58	12.38
Film thickness	15	12	16	15	14

The obtained results indicated that the incorporation of micro/nanofillers of different properties in an appropriate percent induces a decrease in the barrier properties of the composite film. The highest level of barrier capacity was observed for PCL-based composite with NCMA–Fe_3O_4 micro/nanofiller. PCL itself has a low beneficial effect on the improvement of barrier properties. Optical microscopy showed that a non-uniform PCL film does not represent a continuous coating with micrometer range cracking, which had an adverse effect on the barrier properties. The incorporation of native NC improved, *i.e.*, increased the capacity of the coating to control the transport of gases through the formed film. Except for the mechanical integrity of the NC particles (high crystallinity), the presence of hydrophilic OH groups also helped in the creation of more uniform PCL-based films, *i.e.*, better networking of the system due to hydrogen bonding interactions. However, these properties were of limited value for improvement of the barrier properties as the percolation effect could not be achieved using THF

as the solvent. Future work on the optimization of solubility/dispersibility of PCL and NC, and adjustment of the rate of solvent evaporation would be crucial to achieve improvement in barrier properties of the formed film. The exceptionally high tendency for interactions/agglomeration of the NC particles was prevented by the magnetite modification. The improvement of barrier properties was achieved using NC–Fe_3O_4 and NCMA–Fe_3O_4 micro/nanofillers in novel barrier composite films. NCMA–Fe_3O_4 demonstrated better properties than NC–Fe_3O_4, which showed the importance of the contribution of the MA residues. The significance of developed surface area in NC–Fe_3O_4 and NCMA–Fe_3O_4 micro/nanofillers, enabling redox reactions that prevent oxygen transport by chemical reactivity, should be emphasized.

CONCLUSION

A film coating procedure was developed in order to obtain food-packaging materials based on polyethylene coated with nanocellulose nanocomposites. The deposition of nanocellulose and chemically modified nanocellulose composites onto the surface of polyethylene was aimed at improving the barrier and mechanical properties of PE for food packaging applications. The morphological, thermal and barrier properties of low-density polyethylene/polycaprolactone-modified nanocellulose hybrid materials were investigated. Nanocellulose/magnetite (NC–Fe_3O_4) and maleic acid functionalized NC/magnetite (NCMA–Fe_3O_4) nanocomposites were prepared and used as fillers at various concentrations (5, 10 and 15 wt. %) in a polycaprolactone (PCL) layer. The addition of the filler did not unfavorably affect the inherent properties of the polymer, especially its barrier properties. Oxygen permeation measurements showed that the oxygen barrier properties of magnetite enriched PCL film were improved due to the chemical activity of the added material. Most of the investigated films with thicknesses of 9–17 μm showed increased barrier properties and some of them fulfill the requirements for modified atmosphere packaging with oxygen permeability values of 10–20 $cm^3\ m^{-2}\ d^{-1}$. The surface modification of nanocellulose with maleic anhydride seemed to be a promising reaction for increasing the hydrophobicity and obtaining optimal interconnection (intensities of interfacial interaction) between the polymer chains and the functional groups on the nanocellulose surface in order to obtain enhanced barrier properties.

Acknowledgment. The authors acknowledge the financial support from the Ministry of Education, Science and Technological Developments of the Republic of Serbia, Project Nos. III45019 and OI172013.

ИЗВОД

ПРОУЧАВАЊЕ БАРИЈЕРНИХ СВОЈСТАВА ПОЛИЕТИЛЕНСКЕ ФОЛИЈЕ СА СЛОЈЕМ КОМПОЗИТА НА БАЗИ НАНОЦЕЛУЛОЗЕ И МАГНЕТИТА

НЕНАД ЂОРЂЕВИЋ[1], АЛЕКСАНДАР Д. МАРИНКОВИЋ[2], ЈАСМИНА Б. НИКОЛИЋ[2], САША Ж. ДРМАНИЋ[2], МИЛИЦА РАНЧИЋ[3], ДАНИЈЕЛА В. БРКОВИЋ[4] и ПЕТАР С. УСКОКОВИЋ[1]

[1]Катедра за графичко инжењерство, Технолошко–металуршки факултет, Универзитет у Београду, Карнегијева 4, 11120 Београд, [2]Катедра за органску хемију, Технолошко–металуршки факултет, Универзитет у Београду, Карнегијева 4, 11120 Београд, [3]Шумарски факултет, Универзитет у Београду, Кнеза Вишеслава 1, 11030 Београд и [4]Иновациони центар, Технолошко–металуршки факултет, Универзитет у Београду, Карнегијева 4, 11120 Београд

У овом раду су проучаване морфолошке, термалне и баријерне карактеристике полиетиленског/поликапролактонског хибридног материјала на бази наноцелулозе и магнетита. Композити наноцелулоза–магнетит (NC–Fe_3O_4) и малеинском киселином функционализована наноцелулоза/магнетит (NCMA–Fe_3O_4) су припремљени и употребљени као пуниоци у поликапролактонском слоју (PLC) при различитим концентрацијама (5, 10 и 15 мас. %). Поликапролактонски слој са пуниоцима је нанет на површину полиетиленске фолије. Додатак пуниоца не нарушава првобитна својства полимерног слоја, нарочито у погледу његових баријерних својстава. Измерена пропустљивост молекула кисеоника указује на чињеницу да додатак магнетита утиче на побољшање баријерних својства поликапролактона. Код узорака где је на полиетиленску фолију нанет PCL са NCMA–Fe_3O_4 микро/нанопуниоцем је уочено највеће побољшање баријерних својстава, што указује на значај модификације површине наноцелулозе анхидридом малеинске киселине.

(Примљено 17. децембра 2015, ревидирано 10. фебруара, прихваћено 11. фебруара 2016)

REFERENCES

1. T. V. Duncan, *J. Colloid Interface Sci.* **363** (2011) 1
2. E. Fortunati, I. Armentano, Q. Zhou, A. Iannoni, E. Saino, L. Visai, L. A. Berglund, J. M. Kenny, *Carbohyd. Polym.* **87** (2012) 1596
3. A. Dufresne, *Mater. Today* **16** (2013) 220
4. D. Klemm, F. Kramer, S. Moritz, T. Lindström, M. Ankerfors, D. Gray, A. Dorris, *Angew. Chem. Int. Ed*. **50** (2011) 5438
5. Y. Habibi, *Chem. Soc. Rev.* **43** (2014) 1519
6. I. Siro, D. Plackett, *Cellulose* **17** (2010) 459
7. Y. Yue, C. Zhou, A. French, G. Xia, G. Han, Q. Wang, *Cellulose* **19** (2012) 1173
8. B. Ly, W. Thielemans, A. Dufresne, D. Chaussy, M. N. Belgacem, *Compos. Sci. Technol*. **68** (2008) 3193
9. J. B. A. da Silva, F. V. Pereira, J. I. Druzian, *J. Food Sci*. **77** (2012) N14
10. M. Martinez-Sanz, A. Lopez Rubio, J. M. Lagaron, *Biomacromolecules* **13** (2012) 3887
11. G. Siqueira H. Abdillahi, J. Bras, A. Dufresne, *Cellulose* **17** (2010) 289
12. C. J. Zhou, Q. W. Wang, Q. L. Wu, *Carbohyd. Polym*. **87** (2012) 1779
13. F. Li, P. Biagioni, M. Bollani, A. Maccagnan, L. Piergiovanni, *Cellulose* **20** (2013) 2491
14. A. P. Siročić, A. Reščček, M. Ščetar, L. K. Krehula, Z. Hrnjak-Murgić, *Polym. Bull*. **71** (2014) 705
15. E. G. Ahangar, M. H. Abbaspour-Fard, N. Shahtahmassebi, M. Khojastehpour, P. Maddahi, *J. Food Process. Pres.* **39** (2015) 1442
16. J. S. Andrew, D. R. Clarke, *Langmuir* **24** (2008) 8435

17. D. Zhang, X. Wang, L.-J. He, W. Song, Z. Sun, B. Han, J.-X. Li, Q.-Q. Lei, *J. Mater. Sci. Mater. Electron.* **24** (2013) 1796
18. C. Deng, J. Zhao, C.-L. Deng, Q. Lv, L. Chen, Y.-Z. Wang, *Polym. Degrad. Stab*. **103** (2014) 1
19. D. Bondeson, A. Mathew, K. Oksman, *Cellulose* **13** (2006) 171
20. D.-Y. Kim, Y. Nishiyama S. Kuga, *Cellulose* **9** (2002) 361
21. T. S. Anirudhan, S. R. Rejeena, *Sep. Purif. Technol*. **119** (2013) 82
22. G. D. Vuković, A. D. Marinković, S. D. Škapin, M. T. Ristić, R Aleksić, A. A. Perić-Grujić, P. S. Uskoković, *Chem. Eng. J*. **173** (2011) 855
23. DIN 53380, *Prüfung Kunstoffolien*, *Elastomerfolien, Bestimmung der Gasdurchlässigkeit*, 1969
24. W. M. Wang, Z. S. Cai, J. Y. Yu, Z. P. Xai, *Fiber. Polym.* **10** (2009) 776
25. Y. Peng, D. J. Gardner, Y. Han, A. Kiziltas, Z. Cai, M. A. Tshabalala, *Cellulose* **20** (2013) 2379
26. D. Klemm, B. Heublein, H.-P. Fink, H. A. Bohn, *Angew. Chem. Int. Ed.* **44** (2005) 3358
27. A. C. Small, J. H. Johnston, *J. Colloid Interface Sci*. **331** (2009) 122
28. M. J. Richardson, J. H. Johnston, T. Borrmann, *Curr. Appl. Phys*. **6** (2006) 462
29. N. Lavoine, I. Desloges, A. Dufresne, J. Bras, *Carbohyd. Polym*. **90** (2012) 735
30. C. Aulin, S. Ahola, P. Josefsson, T. Nishino, Y. Hirose, M. Osterberg, L. Wagberg, *Langmuir* **13** (2009) 7675
31. K. Syverud, P. Stenius, *Cellulose* **16** (2009) 75
32. G. Rodionova, M. Lenes, Ø Eriksen, Ø. Gregersen, *Cellulose* **18** (2011) 127
33. R. T. Parry, *Principles and applications of modified atmosphere packaging of foods*, Chapman & Hall, London, UK, 1993
34. A. Fendler, M. P. Villanueva, E. Gimenez, J. M. Lagaro, *Cellulose* **14** (2007) 427.